

Radiative Measurements of Pressure Modulator Operation

J. R. DRUMMOND AND A. ASHTON

Department of Physics, University of Toronto, Toronto, Ontario, Canada

15 July 1988 and 19 July 1989

ABSTRACT

The pressure modulator is extensively used in atmospheric measurements but is not well characterized in terms of its spectroscopic operation. A series of measurements on a carbon monoxide radiometer is described and comparisons are made with theoretical calculations for the same conditions. Agreement is found between theory and experiment for normalized cell transmissions. Diode laser spectroscopic measurements are also found to give satisfactory agreement if there is some temperature cycling in the modulator cell. Some variation is found in the absolute measurements of equivalent width. The possible reasons for this discrepancy are discussed.

1. Introduction

The pressure modulator has been employed extensively to measure temperatures and trace gas concentrations in the stratosphere. A recent review by Taylor (1983) gives an overview of the technique and its uses.

Despite extensive use of the technique, there has been comparatively little experimental work performed to verify the operation of the modulator. The radiometric measurements have been related to the quantities being measured, such as atmospheric temperature and composition, by a combination of experimental measurements and theoretical calculations (see, e.g., Drummond et al. 1980). However most of the measurements have been relative rather than absolute. The main reason for the lack of absolute measurements is that the modulator response extends over a considerable region of spectral space, but the effective spectral resolution is very small. Any experimental or theoretical technique used to probe operation must extend over a wide span of scales, typically in the range 10^{-3} cm^{-1} to 10^2 cm^{-1} . Until recently it has only been possible to make radiometric (integrated) measurements of modulator performance and some detailed calculations. The situation has now changed. Spectroscopic systems exist that are capable of resolving a single spectral line while the modulator is in motion, and computer systems are now available that can handle the detailed spectroscopic calculations necessary to relate the radiometric and spectroscopic measurements. This paper describes some initial experiments on a carbon monoxide pressure modulator with the objective of understanding the variations in the filtering effect of the cell from both an experimental and theoretical viewpoint. The eventual aim of this research, which is at present only

in its initial stages, is to explain the operation of a modulator completely without recourse to parameterization or scaling factors.

2. The pressure modulator

A pressure modulator consists of a cell of gas, the pressure modulator cell or PMC, whose pressure is varied cyclically by a piston and cylinder arrangement (Fig. 1). The cycling of pressure, or more accurately the cycling of density, produces variations in the absorption profiles of the spectral lines of the gas in the cell. Radiation passing through the PMC is then also modulated synchronously with the cell cycling if it possesses spectral components at wavenumbers where the absorption is changing; i.e., the radiation is modulated if it has components close to the line centers of the gas in the cell. For atmospheric emission studies the vibration-rotation bands of the gas in the infrared are used and a conventional multilayer filter is used to isolate the desired spectral region (see, e.g., Drummond et al. 1980). The radiation is then allowed to fall on a detector and the component synchronous with the pressure cycling is separated out electronically. The synchronous component is extremely sensitive to the presence of incoming radiation at frequencies near the spectral lines.

As an extension of the pressure modulator technique, a fast chopper is often used ahead of the cell. The frequency separation of the chopper ($\approx 500 \text{ Hz}$) and the cell cycling ($\approx 11 \text{ Hz}$) is sufficient for the overall radiative signal on the detector to be considered as an amplitude modulated wave. The carrier is the overall chopped signal at the chopper frequency, and the sidebands are the effect of the pressure modulator cycling. An example of such a signal is shown in Fig. 2. The advantages of the fast chopper are that the signals due to vibrations and temperature cycling in the modulator

Corresponding author address: Dr. J. R. Drummond, Dept. of Physics, University of Toronto, Toronto, Ontario, Canada M5S 1A7.

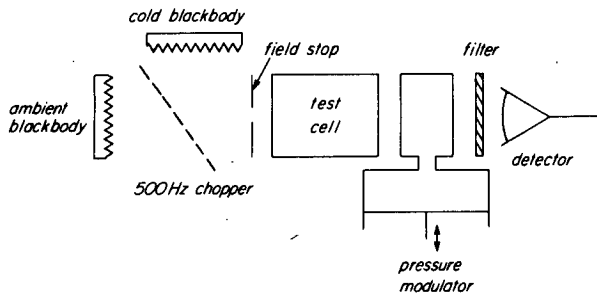


FIG. 1. Schematic of a pressure modulator radiometer as used in these experiments. The cold blackbody is at liquid nitrogen temperature.

cell are eliminated because they only appear at the modulator frequency. Additional benefits are found with some detectors that suffer from elevated low-frequency noise, as the signal is effectively translated upwards to the chopper frequency.

An equivalent and useful description of the effect of a modulator cell and its associated electronics is that of two spectral filters, as shown in Fig. 3. The carrier amplitude or "wideband signal" measures the overall input radiation but suppresses signals from frequencies near cell lines. The sideband amplitude or "sideband signal" only responds to radiation from near cell lines. It should be emphasized that this description of a modulator operation, although correct and useful, is an overall phenomenological description rather than a mechanistic one.

The mechanical construction of a pressure modulator cell may be resonant, with a mechanically determined operating frequency, or nonresonant and internally or externally driven. The constraints and intended

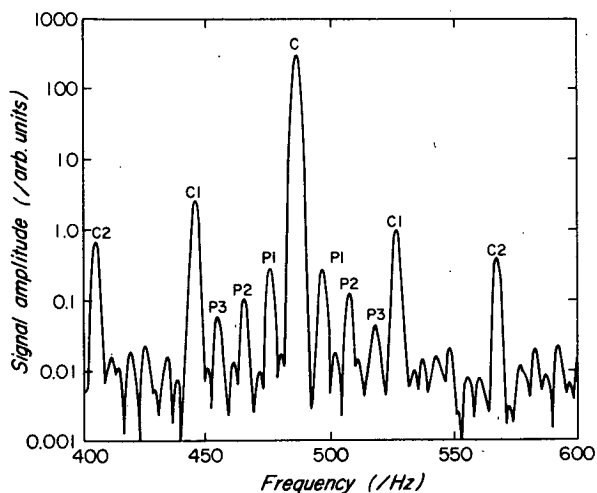


FIG. 2. A Fourier spectrum of the output from the preamplifier in the region of the chopper frequency. Clearly shown are the wideband signal (C) which is modulated at the chopper frequency and the pressure modulator sidebands and their harmonics (P1-P3). Chopper subharmonics (C1-C2) due to the asymmetries in the rotating chopper can also be seen.

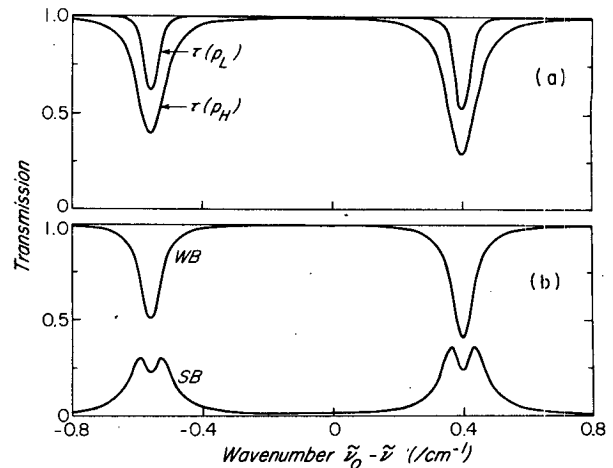


FIG. 3. The operation of a pressure modulator in spectral space. In (a) we show the transmission of the pressure modulator cell for the extreme pressures of the cycle. The equivalent filter profiles (see text) are shown in (b) for the "wideband" (WB) and "sideband" (SB) channels.

usage often determine the form to be used. The modulators used in this study were nonresonant, externally driven modulators used in the University of Toronto Balloon Radiometer (TORBAR) Project (Drummond et al. 1989). The construction of such a modulator is shown in Fig. 4. Since the modulator is driven at a constant rotation rate by the motor, the volume cycling of the cell above the piston is easily calculable. However, as discussed below, the density cycling in the modulator cell may be different.

The objective of these experiments is to determine whether the theory of pressure modulation can be reconciled with measurements, without recourse to parameterization. A gas such as carbon monoxide (CO) offers a number of advantages for these experiments: it is a diatomic gas with a classic P-R spectrum of well-separated lines. Even when isotopes and hot bands are accounted for, this simple picture is essentially maintained. The spectrum is also well determined. A large number of theoretical and experimental studies have elucidated all the major features of the spectrum and their temperature dependencies. A recent study by Nakazawa and Tanaka (1982) gives accurate information on the collision broadening parameters and the line positions. The Air Force Geophysical Laboratories' line compilation (Rothman et al. 1983) lists the strengths and lower energy levels. Thus the basic spectral data are available for theoretical calculations.

3. Transmission measurements

Since the pressure modulator is used to measure gas concentrations outside the modulator cell, a natural measurement is the sensitivity of the modulator to gas contained in a test cell in the configuration shown in Fig. 1. The basic radiometric signal from the modulator is given by

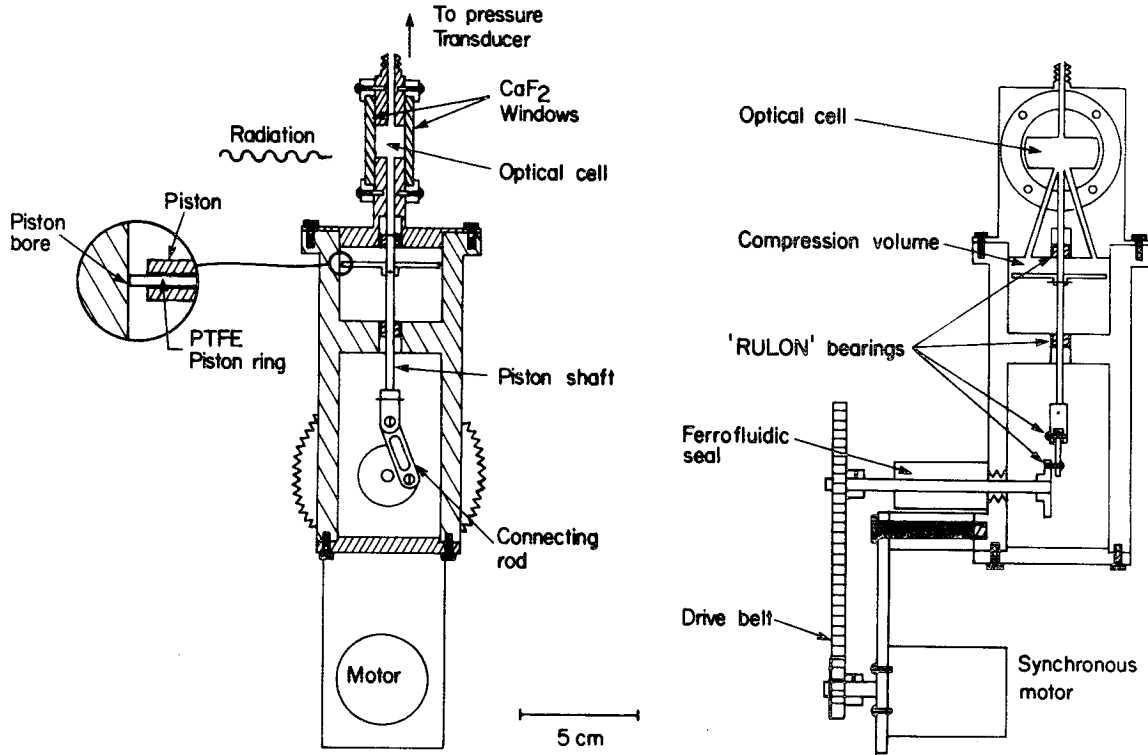


FIG. 4. Mechanical drawing of a pressure modulator system as used for these experiments. The gas pressure is modulated using a piston and connecting rod system not unlike an automobile engine. Drive power is transferred through the vacuum wall by a Ferrofluidic seal (Ferrofluidic Corp.). The bearings are made of plastic (RULON from Dupont Corp.).

$$R(t) \propto \int_{\tilde{\nu}} B(\tilde{\nu}, T_{bb})\tau_f(\tilde{\nu})\tau_a(p_a)\tau(p_c(t), T_c(t))d\tilde{\nu},$$

where $R(t)$ is the radiation incident upon the detector as a function of time, $B(\tilde{\nu}, T_{bb})$ the blackbody radiation from the ambient blackbody at temperature T_{bb} , τ_f the filter transmission, τ_a the test cell transmission, and $\tau(p_c, T_c)$ the instantaneous PMC transmission at pressure p_c and temperature T_c . It is assumed that the emission from the liquid-nitrogen cooled reference blackbody is negligible.

The modulated radiative signal is converted to an electrical signal by the detector. After processing in the electronics by filtering, phase-sensitive detection, and integration, two electrical signals are produced. One of these, S_w , is related to the wideband signal, the other, S_s , to the sideband signal. The relationships between the electrical signals and the optical properties are given by

$$S_w = G_w \int_{\tilde{\nu}} B(\tilde{\nu}, T_{bb})\tau_f(\tilde{\nu})\tau_a(p_a)\overline{\tau(p_c(t), T_c(t))}d\tilde{\nu}$$

$$S_s = G_w K_s f \int_{\tilde{\nu}} B(\tilde{\nu}, T_{bb})\tau_f(\tilde{\nu})\tau_a(p_a) \times [\tau(p_l, T_l) - \tau(p_h, T_h)]d\tilde{\nu},$$

where G_w is the electronic gain of the wideband channel and K_s accounts for the relative electronic gains of the two channels and the phase-sensitive detector. The subscripts h and l refer respectively to the high and low extremes of the cell cycle. The overbar indicates a time average. The factor f relates the effect of the actual modulation waveform to the peak-to-peak calculation of the integral using the pressure modulator pressure transducer values assuming isothermal operation. The use of a constant factor is permitted because the ratio between the peak-to-peak calculation and a full analysis of the cycle is found to be constant for all the cases considered. The parameter f is discussed further below.

In order to eliminate the effects of changes in the blackbody temperature and other thermal drifts on the experiment, the ratio S_s/S_w is taken. Since the wideband PMC transmissions are nearly unity over the range of the filter profile, the denominator is a measure of the total radiation from the blackbody rather than a measure of any test cell conditions. To further simplify the results the ratio is normalized to the ratio for an empty test cell

$$X(p_a) = \frac{S_s(p_a)/S_w(p_a)}{S_s(0)/S_w(0)}.$$

The function X is then like transmission in that it is bounded by unity for an empty test cell and zero for

a test cell containing an infinite amount of gas. It is often referred to as the "PMC transmission" of the test cell.

Laboratory experiments are performed with either pure gas or a gas mixture, usually with nitrogen as the second gas. The objective is to probe the variation of absorption at various density-pressure combinations in the test cell and compare the experiments with theoretical calculations. The principal difference expected is a result of the variation in collision-induced line-widths between self-collisions, which predominate in the pure gas and concentrated mixtures, and foreign collisions, which predominate at high dilution. Since the atmosphere is a "high dilution" case (typical stratospheric concentrations are in the range 10–100 ppbv) and the PMC is a "pure gas" case, both extremes are relevant to a real atmospheric experiment.

In a typical experimental run pure gas is admitted to the test cell until a desired pressure is reached, and then nitrogen is admitted to change the pressure without changing the CO density. Considerable care has to be exercised to ensure that the gas concentrations are known and that they are completely mixed in the test cell. Further details of these experiments are given in Ashton (1985).

The results for a typical run are shown in Fig. 5 along with theoretical calculations that match the experimental conditions. As can be seen from the diagram, the agreement between theory and experiment, for both pure carbon monoxide and CO/nitrogen mixtures, is within the experimental error, which is due to the noise levels on the signals, the accuracy of the 0% and 100% levels, and the calibration of the pressure transducers. We have found agreement between calculation and experiment for all cases examined, with the exception of very high amounts of CO and high modulator pressures where there is some difference between the calculations and the experimental results. These high amounts are not of direct atmospheric relevance since they are unrealistically high, but will be studied in the future to resolve the discrepancy.

The apparent success of the above measurements is somewhat deceptive because the normalization techniques used to reduce the sensitivity to temperature variations also reduce the sensitivity of the experiment to the absolute values of the spectroscopic line parameters and other data. In particular, the electronic gains and the factor f are eliminated. In order to consider these parameters further it is necessary to examine the modulator operation in more detail. A major impediment to such an analysis is the lack of knowledge concerning the exact pressure cycling in the cell. From a theoretical standpoint it is clear that the actual cycling in the cell may be characterised as isothermal, adiabatic, or intermediate between these extremes depending upon the construction, compression ratio, and operating frequency of the cell. Various studies have attempted to model the modulator operation (Schofield 1980) and some progress has been made in the exper-

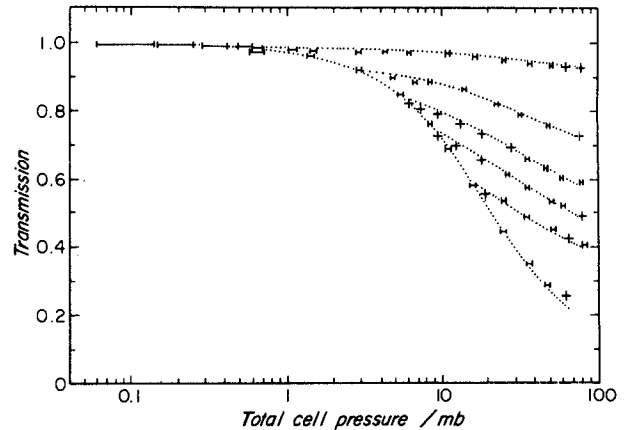


Fig. 5. The results of a laboratory experiment to determine the effective transmission of a cell of CO as viewed by the pressure modulator instrument. The lowest dotted line and data are the results for pure CO in the 21.2 mm long test cell and the "branches" show the effect of adding nitrogen to a CO amount given by the "fork" point in the curve. The dotted line is computed using the general overlapping line-by-line model given the cell and modulator conditions. The experiment was performed at 300 K with modulator pressure extremes of 20.9 and 8.5 mb, and a 10 mm modulator path.

imental field (Ballard 1979). However, it is not a simple task to measure the pressure cycling of a PMC during operation.

Early modulators, such as those used for the Nimbus 6 PMR and Nimbus 7 SAMS instruments (see Taylor 1983), did not attempt to measure the pressure cycling directly. The fact that the operating frequency of a resonant modulator varies with the mean gas pressure, which alters the effective spring constant in the system, was used as a pressure measurement system. A calibration of pressure versus frequency is then performed using known mean pressures and a calibration table can be set up for later use (Drummond et al. 1980). However, this procedure cannot be used for nonresonant systems such as those used for the TORBAR instrument and a pressure sensor is required.

Any pressure sensor attached to the system will add plumbing and volume, disturbing the system somewhat. Thus any measurement must be simultaneous with the radiometric measurements. In addition the sensor must have a fast enough response to follow the pressure variations. In our apparatus we use a Validyne AP10 absolute gauge, produced by Validyne Corporation, which operates on the variable reluctance principle and has a fast response. However, the sensor is mounted at the end of a small tube of complex cross-section (see Fig. 4) and, although laminar flow calculations show that the lag at the end of the pipe is small, we appear to see some effect attributable to this configuration (see below).

Neither the resonant technique, nor the sensor system, account for the temperature cycling in the cell. This is significant because the modulator is more nearly a "density modulator" than a "pressure modulator."

Our modulator is not thermally controlled but its operating temperature differs negligibly from ambient temperature during operation. This, however, does not imply that the gas is isothermal, as the system is dynamic with alternate compression and rarefaction cycles—the modulator body temperature would only represent an average temperature over the cycle. In order to probe the gas temperature a system is required that can measure the cell density cycling remotely. Diode laser spectroscopy offers this possibility.

4. Diode laser scanning measurements

Diode laser spectroscopy offers the possibility of performing Doppler-limited resolution studies with high time resolution. In simplest terms a diode laser is a monochromatic infrared source whose frequency may be scanned over a small spectral region by varying the diode current. Diode lasers have been widely applied to high-resolution spectroscopy, in particular to studies of spectral line strengths and widths. They have also been widely used in atmospheric studies for trace gas detection in the troposphere (Hastie et al. 1983). In the present application they offer the possibility of directly measuring an absorption line profile under dynamic conditions. A brief report on some measurements with a resonant modulator has been presented by May et al. (1988).

There are some problems with diode laser techniques. The major ones for the purpose of this study are those of multimode operation and frequency stability. Multimode operation implies that there is more than one longitudinal laser mode active simultaneously. The most noticeable effect is that the transmission at a line center falls to a constant nonzero value as the absorber amount increases. These additional modes may be corrected for by using the line center as a 0% transmission point under conditions of high absorber amount. Lack of frequency stability implies that the line center will apparently shift even with consistent scanning parameters. This effect is particularly noticeable in our apparatus because the data gathering is intermittent and the cell conditions are changing asynchronously with the spectral scanning (see below). Special provision has to be made in the data averaging system to account for this drift.

The basic experimental layout is shown in Fig. 6. The apparatus is a simple transmission system with a computerized scanning and data collection system. No effort was made to synchronize the operation of the modulator with the scanning of the diode laser, with the result that some considerable data sorting had to be performed after the experiment. The sorting was done in conjunction with a correction for the drift in line center position yielding a uniform set of line profiles at specific points in the modulator cycle. Scanning to 0.1 cm^{-1} from the line center of the R2 line of $\text{C}^{12}\text{O}^{16}$ at $2154.5959 \text{ cm}^{-1}$ was obtained by varying the diode current while keeping the temperature stable.

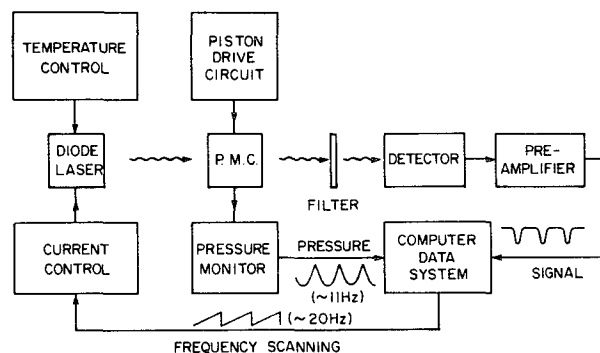


FIG. 6. Layout of the diode laser experiment to measure the absorption profile of a single line while the PMC is operating. The computer provides the scanning signal and monitors the pressure and signal. Since the frequency scanning and pressure modulation are asynchronous the data must be sorted after the experiment to obtain "slices" of the modulator operation at various times in the cycle.

Calibration information was supplied from experiments performed with the modulator at rest yielding a static profile. From this profile estimates of the 0% and 100% lines and the scan rate could be made. The best-fit scan rates were consistent for all the static pressures used in the cell and the 0% and 100% points varied in a manner consistent with small experimental drifts. An example of a static line profile and the best-fit data are shown with the residuals in Fig. 7. While it may be seen that the fit is not perfect, it is found to be more than adequate for the purposes of these experiments.

The results from an experimental run were plots of recorded transducer pressure versus time in a cycle, and line profiles measured at 128 different transducer pressures for both the compression and rarefaction phases of the cycle—a total of 256 line profiles. These experiments were repeated at three different mean modulator pressures (6.4, 15.3, and 20.1 mb) to cover a range of operating conditions.

Fitting a line profile to the data should involve matching, in a least-squares sense, the pressure and temperature of the cell gas using the basic spectroscopic data and a voigt line profile. In practice the fitting of the line is more accurately described as a fitting to density, with second-order effects due to temperature and pressure. The lack of sensitivity to temperature cycling is not unexpected, but means that we are unable to unambiguously determine both temperature and pressure from the measurements. Accordingly, some assumption about the interrelation between the two must be made.

Two cases are immediately apparent: isothermal and adiabatic. These may be represented as $T = T_0(p/p_0)^b$ where $b = 0.0$ for the isothermal case and $b = 2/7$ for adiabatic conditions. As an attempt to consider intermediate conditions we allow b to be a variable with extrema of 0 and $2/7$.

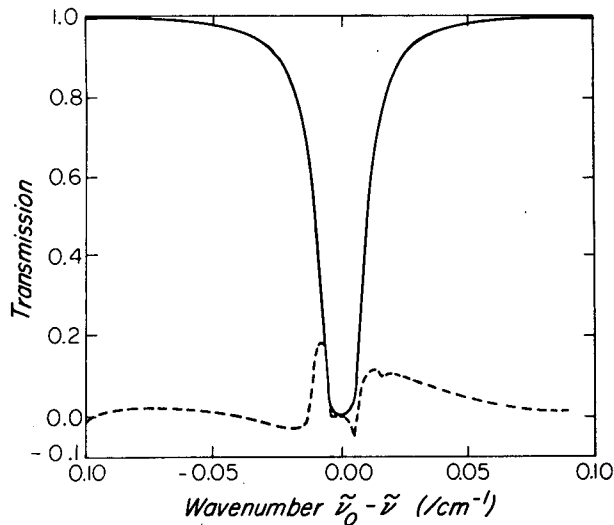


FIG. 7. A comparison of the theoretical and experimental profiles of the R2 line under static conditions. The difference between the two profiles is shown on a 10 \times scale as the dashed line. The static cell pressure is 20 mb.

The problem of fitting the profiles with a chosen value of b is now a one-dimensional minimization problem that may be readily accomplished for all points on the cycle. The results in terms of pressure cycling are shown for one case in Fig. 8 along with the recorded pressure from the transducer. The results show that the pressure peak as deduced from the diode laser data using any value of b precedes the peak as recorded from the transducer, implying some lag in the transducer system comprising the plumbing, mechanics, and electronics. The lag is of the order of 0.05 of a cycle or 20°. If the lag is a conventional first-order lag then one would expect that the pressure peak recorded by the transducer would be less than that deduced from the diode laser system by some 6%, but this is not the case for the isothermal calculation from the diode laser data. In fact it can be seen that, unless there is an unknown resonance effect, the isothermal conditions produce nonphysical results. Inspection of the pressure modulator mechanism in Fig. 4 shows that the pressures in the space above the piston, p_p , in the actual modulator cell, p_c , and in the transducer, p_t , would be expected to be in sequence; i.e., $p_p > p_c > p_t$ or $p_p < p_c < p_t$ over the majority of the compression and rarefaction cycle respectively. However, Fig. 8 shows otherwise, particularly for the peak values. While the possibility of a resonance effect cannot be ruled out, a much more probable explanation is that the gas is temperature cycling.

In a fully adiabatic model the gas temperatures are extreme. For example, for the conditions of test 5 (see Table 1), assuming that the gas is at 296 K at the mean pressure, the temperature extrema are 252 K and 360 K, a temperature cycle of over 100 K. In that case we would expect to see very significant thermal emission

signals from the cell. We have attempted to observe such emission but, although there is a signal present, it is too small to reliably measure. Calculations show that the small emission signal would indicate temperature cycling of the order of 10 K rather than 100 K. Temperature cycling of this order of magnitude is also more in agreement with the modeling studies of Schofield (1980). The approximation of some temperature cycling may be studied by setting $b = 0.1$ in our p - T relationship giving the intermediate results shown in Fig. 8, which satisfy the intuitive ideas of pressure relationship already discussed, as well as reasonable temperature swings. Thus, while not in any sense quantitative, the results are consistent with a small temperature swing in the modulator.

The measurements of density cycling obtained above can be most easily related to the integrated radiometric equations through the factor f . The factor f relates the results of the actual modulation waveform to the peak-to-peak calculation of the integral using the pressure-modulator pressure-transducer values. All other quantities such as line strengths, gains, etc. are measurable by completely separate experiments by ourselves or other groups. For a sinusoidal modulation at an amplitude of $(\tau(p_i) - \tau(p_h))/2$ the value of f is defined to be unity, and for a square wave it would be $4/\pi$ as the electronics selects only the fundamental frequency of the modulated waveform. We can therefore perform a Fourier analysis of the radiometric signal corresponding to the density cycle obtained above and take the ratio

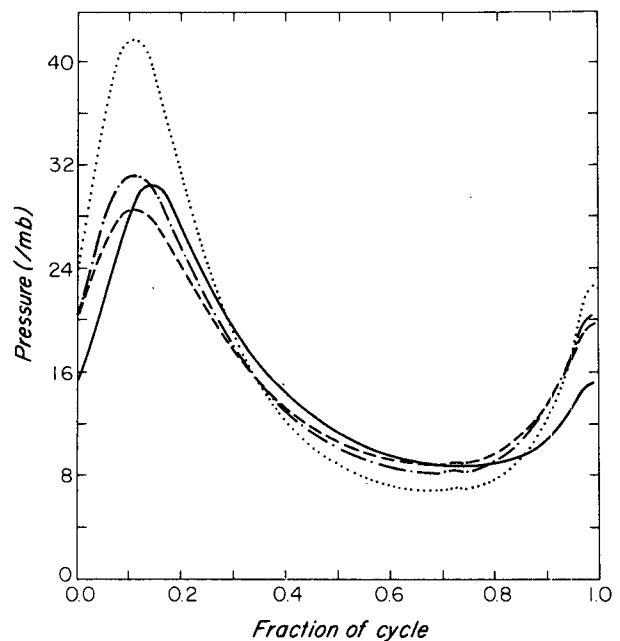


FIG. 8. The pressure cycle for the modulator measured by the pressure transducer as a function of time along the cycle (solid line). The other lines represent the pressures derived from the line shape for the same dataset using isothermal (dashed line), $b = 0.1$ (dash-dot line), and adiabatic (dotted line) assumptions to relate pressure and temperature.

TABLE 1. Values of the factor f derived from the diode laser scanning measurements. In cases where two values of f are quoted, the upper value assumes that the gas is at 296 K at the static pressure, and the lower value assumes that the gas is at 296 K at the trough pressure.

| Test number | Pressure (mb) | | | f | | | Transducer |
|-------------|---------------|------|--------|-----------|--------------|--------------|------------|
| | Static | Peak | Trough | $b = 0.0$ | $b = 0.1$ | $b = 2/7$ | |
| 4 | 6.4 | 12.1 | 4.4 | 0.83 | 0.84 0.85 | 0.86 0.90 | 0.82 |
| 5 | 15.3 | 30.5 | 8.7 | 0.80 | 0.80 0.85 | 0.90 1.00 | 0.82 |
| 6 | 20.1 | 40.7 | 11.3 | 0.74 | 0.76 0.78 | 0.83 0.93 | 0.81 |

of the first harmonic to half the peak-to-peak value, which gives an alternative evaluation of the factor f . However, since the radiometric signal is found to be linearly related to the density over the range of pressures used here, an equivalent operation is the analysis of the density cycling itself. This can then be compared to the value obtained by direct analysis of the pressure cycling and further experiments described below.

The results are shown in Table 1 in terms of the factor f for various assumptions about the cell conditions. The derived value of f is not very sensitive to the value of b used; therefore no conclusions regarding temperature cycling can be drawn from this analysis. The values of f are also consistent with the pressure transducer values but lie somewhat below the value of 0.89 calculated from a sinusoidal piston movement, equalized pressure and temperature throughout the volumes, and no gas flow past the piston seal. A value below this is entirely reasonable as the gas losses alone would cause the value of f to drop. The error on the value of f is small but difficult to quantify without statistics from a larger set of experiments that are not yet available. The error is mainly due to the accuracy of the fitting of the line profiles to the density. The reason for this is that most systematic errors, such as the pressure transducer calibration, cancel in the ratios taken to determine f . The random contribution is fairly small ($\pm 2.5\%$) and comes mainly from the pressure transducer system. Additional small errors come from the quantization errors of the digitizer and the Fourier analysis. The accuracy of the fitting may be seen in Fig. 8 where the "noise" from fitting adjacent points is small but visible. A more significant problem in determining the true value of f is the necessity of assuming a value of b in the p - T relationship.

As the pressure rises the discrepancy between the pressure transducer value and the diode laser measured value increases. The reasons for this, as discussed above, are twofold: (i) The pressure transducer does not measure the cell pressure cycling but lags somewhat behind, and (ii) the gas in the cell undergoes temperature cycling. Unfortunately we cannot isolate the two effects other than by the consistency arguments on pressure and thermal emission discussed above. These lead to the conclusion that the true adiabatic cycle is unreasonable, even for the highest pressures, but that an in-

intermediate state between isothermal and adiabatic (see Fig. 8) would be consistent with the various arguments.

5. "Equivalent width" measurements

If a radiometric measurement is made with an empty test cell and normalized to the wideband signal, the factor f may be determined by comparing the results of the experiment to the theoretical calculation:

$$\frac{S_s(0)}{S_w(0)} = K_s f \times \frac{\int_{\tilde{\nu}} B(\tilde{\nu}, T_{bb})\tau_f(\tilde{\nu})\tau_a(p_a)[\tau(p_l, T_l) - \tau(p_h, T_h)]d\tilde{\nu}}{\int_{\tilde{\nu}} B(\tilde{\nu}, T_{bb})\tau_f(\tilde{\nu})\tau_a(p_a)\overline{\tau(p_c(t))}d\tilde{\nu}}$$

Using the modulator system and an empty test cell the ratio $S_s(0)/(S_w(0)K_s)$ was measured for various cell pressures and compared to the integrated ratio. The

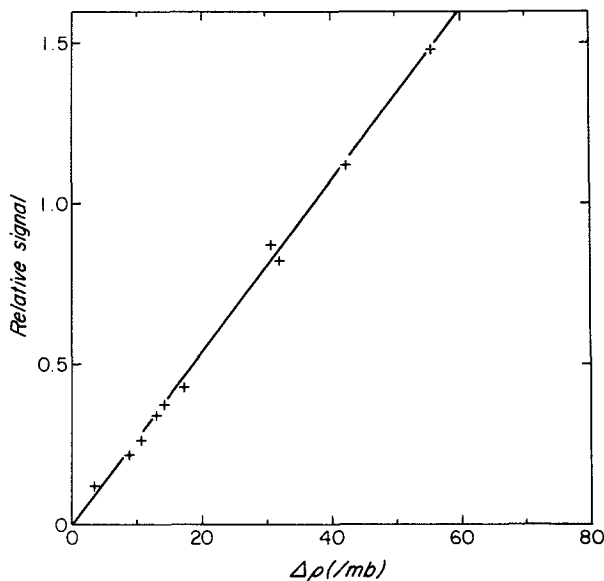


FIG. 9. The results of a radiometric determination of the factor f as a function of the difference in pressure extremes (as measured by the transducer) in the PMC. The value of f derived from the slope of the solid line (see text) is 0.62 ± 0.02 .

results, shown in Fig. 9, yield a value for f of 0.62 ± 0.02 . The calculation of the integral ratio was performed using a full overlapping line calculation with the AFGL data (Rothman et al. 1983) for line positions, strengths, and energy levels supplemented with the data of Nakazawa and Tanaka (1982) for the self-broadened halfwidth. The errors shown in Fig. 9 are due to signal to noise ratios and pressure transducer calibration. The accuracy of the calculation is limited by our knowledge of the line parameters, assuming that the fundamental line-shape theory is correct. The error from this source is about 1% (Nakazawa and Tanaka 1982).

A single-point measurement of the integral ratio was also made more directly by digitizing the output of the detector preamplifier, performing a Fourier transform of the result (see Fig. 2), and then examining the side-band ratios directly. This measurement confirms the experimental values quoted above, thus indicating that the operation of the electronics system is properly understood.

6. Discussion

The three sets of experiments described above give varying but consistent views of modulator operation. Since this is the first complete series of experiments specifically aimed at comparing theoretical predictions and experimental results for the modulator itself, this is very satisfying. The transmission measurements reported in the first part show agreement between the theory and experiment within the limits of the experimental error. The diode laser measurements show a coherent view of a modulator undergoing a small amount of temperature cycling during operation. The line shapes agree well with a simple collision-broadened shape. Since these are the experiments most directly related to the operation of a field instrument, our confidence in predicting instrument performance is increased.

The only significant discrepancy is between the values of f deduced from the diode laser measurements (0.76 – 0.85) and that from the radiometric measurement 0.62 ± 0.02 . The diode laser system measures the line profile cycling for the R2 line of $C^{12}O^{16}$ only, but the "equivalent width" experiment measures an integrated signal over the whole band using a different experimental system. A possible explanation is therefore some error in measuring the experimental conditions. A more detailed set of experiments is therefore called for in which the spectroscopic and radiometric measurements are combined. A useful extension of the experiment, which is unfortunately not possible with

the present equipment, would be to measure two lines with different temperature variations. A two-parameter fit might then be possible; however, this would require two simultaneous measurements—a difficult task. Finally the ideal experiment would be to scan the whole filter profile at Doppler-limited resolution.

7. Conclusions

Measurements of pressure modulator transmission for a carbon monoxide modulator observing pure CO and CO/nitrogen mixtures agree with calculations based on spectroscopic line data within the limits of the experimental error.

The pressure cycling of a carbon monoxide modulator has been observed directly. The results show reasonable agreement with the radiometric measurements but the residual differences are outside the estimated errors of the two experiments. Further experiments are required to resolve these problems.

Acknowledgments. The diode laser experiments were performed at the National Center for Atmospheric Research with the assistance of Dr. A. Fried, Dr. W. Mankin, and Dr. P. Sperry of the Atmospheric Chemistry Division. This work was supported by the National Science Research Council of Canada.

REFERENCES

- Ashton, A., 1985: Stratospheric measurements of CO concentration. M.S. thesis, University of Toronto, 121 pp.
- Ballard, J., 1979: Studies of some trace gases in the stratosphere and mesosphere. Ph.D. thesis, University of Oxford, 129 pp.
- Drummond, J. R., D. Turner and A. Ashton, 1989: A pressure modulator radiometer for measuring stratospheric trace gases. *Rev. Sci. Instrum.*, **60**, 3522–3532.
- , J. T. Houghton, G. D. Peskett, C. D. Rodgers, M. J. Wale, J. Whitney and E. J. Williamson, 1980: The stratospheric and mesospheric sounder on Nimbus 7. *Phil. Trans. Roy. Soc. London*, **A296**, 219–241.
- Hastie, D. R., G. I. Mackay, T. Iguchi, B. A. Ridley and H. I. Schiff, 1983: Tunable diode laser systems for measuring trace gases in tropospheric air. *Environ. Sci. Technol.*, **17**, 352A–364A.
- May, R. D., D. J. McCleese, D. M. Rider, J. T. Schofield and W. R. Webster, 1988: Tunable diode laser spectral diagnostic studies of a pressure modulator radiometer. *Appl. Opt.*, **27**, 3591–3593.
- Nakazawa, T., and M. Tanaka, 1982: Intensities, half-widths and shapes of spectral lines in the fundamental band of CO at low temperatures. *J. Quant. Spectrosc. Radiat. Transfer*, **28**, 471–480.
- Rothman, L. S., A. Goldman, J. R. Gillis, R. R. Gamache, H. M. Pickett, R. L. Poynter, N. Husson and A. Chedin, 1983: AFGL trace gas compilation: 1982 version. *Appl. Opt.*, **22**, 1616–1626.
- Schofield, J. T., 1980: The remote sounding of the Venus atmosphere. Ph.D. thesis, University of Oxford, 307 pp.
- Taylor, F. W., 1983: Pressure modulator radiometry, in spectroscopic techniques, Vol. III., Academic Press, 137–198 pp.